AJNR

Atypical skull base paragangliomas.

E R Noble, W R Smoker and N R Ghatak

AJNR Am J Neuroradiol 1997, 18 (5) 986-990
http://www.ajnr.org/content/18/5/986

Atypical Skull Base Paragangliomas

Edward R. Noble, Wendy R. K. Smoker, and Nitya R. Ghatak

Summary: We present two cases of unusually large skull base paragangliomas. The first tumor was accompanied by marked bony destruction of the central skull base and multiple associated cysts. The second tumor arose along the petrous ridge, with a large intracranial component. The CT, MR imaging, angiographic, histologic, and electron microscopic findings of these unusual lesions are described.

Index terms: Paraganglioma; Skull, neoplasms

Paragangliomas are tumors that arise from paraganglion cells of the parasympathetic system, cells of neural crest origin. Paraganglioma of the head and neck was reported in 1862 by Von Luschka, who described a carotid body tumor (1). In the head and neck, the most common locations for paragangliomas are the carotid bifurcation, the jugular bulb, and the middle ear. Paragangliomas have been described in many locations in which paraganglionic tissue is not normally located, including the sella and parasellar regions (1–3). The first case we describe is unusual because of the extensive involvement of the central skull base and its heterogeneous cystic/solid composition. The second case is that of a very large tumor arising along the petrous ridge and extending intracranially.

Case Reports

Case 1

A 71-year-old man began to notice a change in his peripheral vision when fixing his boat dock. On physical examination he was found to have bilateral optic atrophy, bitemporal hemianopsia, and anosmia. The remainder of his cranial nerves were intact and no endocrinologic disturbance was detected. A computed tomographic (CT) scan obtained at an outside hospital showed an enhancing mass with extensive destruction of the central skull base and clivus. A biopsy of the mass was done, and the initial pathologic report was meningioma.

The patient came to our institution for additional evaluation. Arteriography showed a vascular mass involving the region of the sella, encasement of both internal carotid arteries, displacement of the basilar artery, and tumor blush in the region of the central skull base and right orbital apex (Fig 1A–C). A repeat CT study and magnetic resonance (MR) imaging were performed, at which time the mass was seen to replace all of the central and a portion of the anterior skull base, severely compressing the brain stem and displaying heterogeneous enhancement (Fig 1D–I). Multiple associated cysts were seen at the margins of the mass, some with the intensity of cerebrospinal fluid and others with shortened T1 and prolonged T2 relaxation times. The diagnosis of meningioma was questioned.

A right frontotemporoparietal craniotomy was performed. Several large cysts containing "crankcase-type" fluid were encountered during resection of the temporal tip. The mass was found to encase major vessels, the optic nerves, and the optic chiasm. A partial resection of the mass was performed to relieve compression of the optic nerves, chiasm, and brain stem.

The tumor was studied by using various staining methods, including immunohistochemistry for chromogranin, S-100 protein, cytokeratin, and the following pituitary hormones: prolactin, growth hormone, corticotropin, thyrotropin, follicle-stimulating hormone, and luteinizing hormone. In some areas of the tumor, the cells were arranged in clusters best seen in reticulin-stained sections (Fig 1J). In other areas, they were arranged in a linear or trabecular fashion. Most tumor cells displayed strong reactivity for chromogranin. A variable number of supporting cells throughout the tumor showed positive reaction for S-100 protein. The tumor cells showed no reaction for any pituitary hormones or cytokeratin.

Case 2

The second patient, a previously healthy 14-year-old boy, had a 1-month history of headaches, vomiting, unsteady gait, and personality changes. The headaches were right-sided and associated with right-sided facial pain. Physical examination revealed a palsy of right cranial nerve VI, mild right-sided hearing loss, and unsteady gait.

Received August 24, 1995; accepted after revision October 4, 1996.

From the Departments of Radiology (E.R.N., W.R.K.S.) and Pathology (N.R.G.), Medical College of Virginia, Richmond.

Address reprint requests to W. R. K. Smoker, MD, Department of Radiology, Medical College of Virginia, 1200 E Marshall St, Box 980615, Richmond, VA 23298-0615.

AJNR 18:986–990, May 1997 0195-6108/97/1805–0986

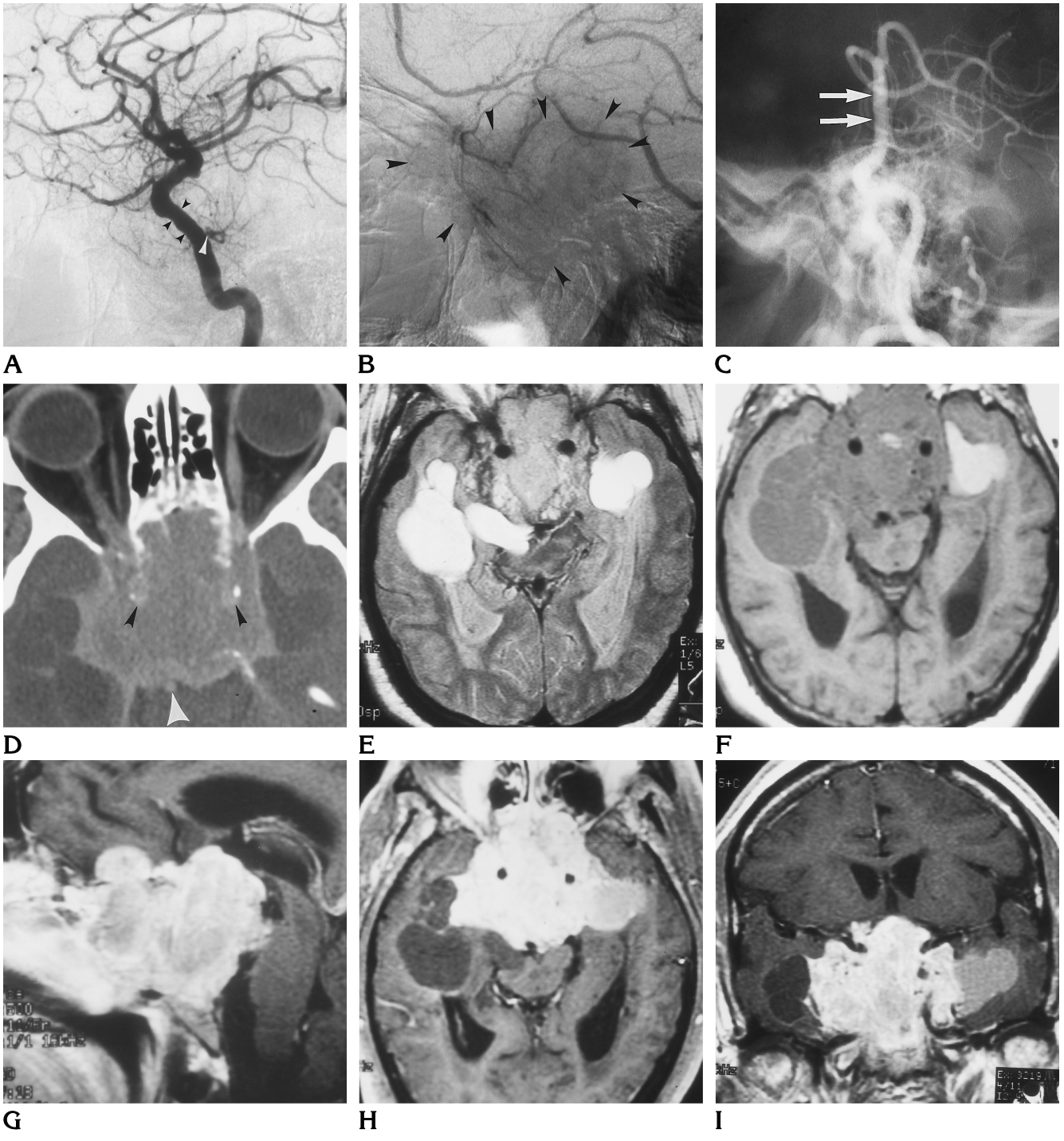

Fig 1. A 71-year-old man with enhancing mass accompanied by extensive destruction of the central skull base and clivus.

Arterial (*A*) and venous (*B*) phase lateral views from a left internal carotid artery angiogram show a vascular mass supplied by branches of the meningohypophysial trunk (*white arrowhead, A*). The lesion appears to encase the carotid artery (*black arrowheads, A*). A homogeneous blush persists late into the venous phase (*arrowheads, B*).

C, Lateral view from a left vertebral arteriogram shows marked posterior displacement of the basilar artery (*arrows*). The sella, dorsum sella, and clivus cannot be defined.

D, Axial CT scan obtained after the angiographic study reveals a huge, centrally solid, faintly enhancing mass with peripheral cystic components involving the central skull base, destroying the clivus and sella, extending into both cavernous sinuses, encasing the internal carotid arteries (*black arrowheads*) and orbital apices, and compressing and displacing the midbrain and basilar artery posteriorly (*white arrowhead*).

Axial fast spin-echo (4000/17/1 [repetition time/echo time/excitations]) (*E*), axial T1-weighted spin-echo (450/141) (*F*), and sagittal (500/11/2) (*G*), axial (350/14/2) (*H*), and coronal (500/11/2) (*I*) contrast-enhanced T1-weighted spin-echo MR images optimally show the marked heterogeneity of this lesion and the intense enhancement of the solid central component, which replaces all of the central skull base. Matrix is 512 × 256 in *E*, 256 × 192 in *F* through *I*. *Figure continues.*

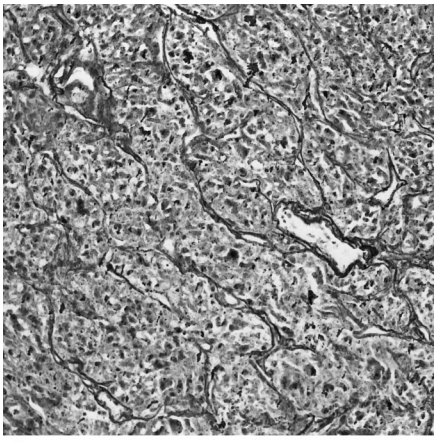

J

Fig 1, *continued*. *J*, Histologic section reveals multiple bundles (clusters) of tumor cells (zellballen), each bundle outlined by reticulin (silver stain for reticulin, original magnification ×200).

The remainder of his physical examination was normal, although he was somewhat lethargic.

CT and MR studies revealed a large, enhancing mass along the right petrous ridge. The mass extended intracranially, compressing the brain stem and showing intense, homogeneous enhancement (Fig 2A–D). Angiography revealed early and persistent tumor blush over the right petrous ridge with marked displacement of posterior circulation vascular structures, although the tumor was supplied by the right anterior circulation (Fig 2E–G).

After placement of a right frontal ventriculostomy, a right suboccipital craniectomy was performed. The seventh and eighth cranial nerves were adherent to the inferoposterior capsule of the tumor, which, when incised, was found to be quite vascular. The bulk of the tumor was removed with suction and the capsule collapsed on itself. The tumor was also adherent to the brain stem medially and to the cerebellum inferiorly. Part of the capsule was removed and the cavity was cauterized and filled with biofibular collagen.

Fig 2. A 14-year-old boy with a 1-month history of headaches, vomiting, unsteady gait, and personality changes.

A and *B*, Axial CT scans before (*A*) and after (*B*) contrast enhancement reveal a slightly hyperdense lesion that enhances dramatically and homogeneously. Note the marked displacement of the basilar artery (*arrowhead, B*).

C and *D*, Contrast-enhanced T1-weighted (700/20/2) MR images in the axial (*C*) and coronal (*D*) planes also reveal a solid, fairly homogeneously enhancing mass centered along the right petrous apex with extension into the posteroinferomedial aspect of the right middle cranial fossa, accounting for the slight asymmetry and elevation of the right temporal horn (*arrowhead, D*). *Figure continues.*

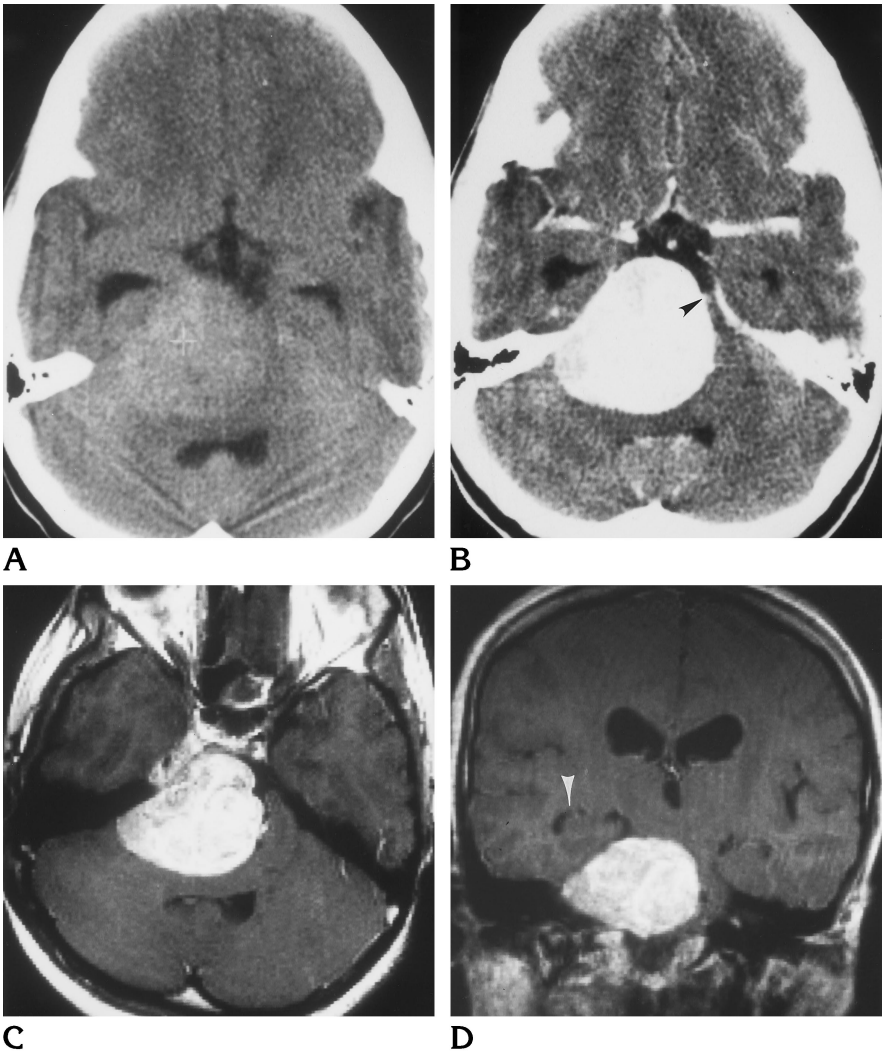

A B C D

In addition to the staining methods used in case 1, we also used electron microscopy to study this tumor. In most areas, the tumor cells were arranged in clusters, closely associated with vascular spaces (Fig 2H). A relatively small number of tumor cells showed a positive reaction for chromogranin. The supporting cells, especially at the periphery of the cell clusters, showed a positive staining reaction for S-100 protein. Electron microscopy showed typical membrane-bound secretory granules within the tumor cells (Fig 2I). The tumor was negative for pituitary hormones.

Discussion

Classically, paragangliomas are highly vascular lesions that can be very destructive. They typically exhibit flow voids on MR images, producing a characteristic "salt-and-pepper" appearance, and are highly vascular on angiographic studies, classically supplied by the ascending pharyngeal artery. Flow voids were not observed on MR studies in either of our cases, which we attribute to their being supplied predominately by the small dorsal clival meningeal branches of the meningohypophysial trunk rather than by the larger vessels that supply the more common jugular paragangliomas (ie, ascending pharyngeal artery).

Rarely, paragangliomas have been reported to involve the sella and parasellar regions: one reported case seems to have shown evidence of lytic destruction of the central skull base (2–4). Our first case is distinctly unusual because of the associated cysts. The second case is unusual by virtue of its location along the petrous ridge with its associated large intracranial component. Otherwise, this tumor had features more typical of classic paragangliomas.

The diagnosis of paraganglioma in both

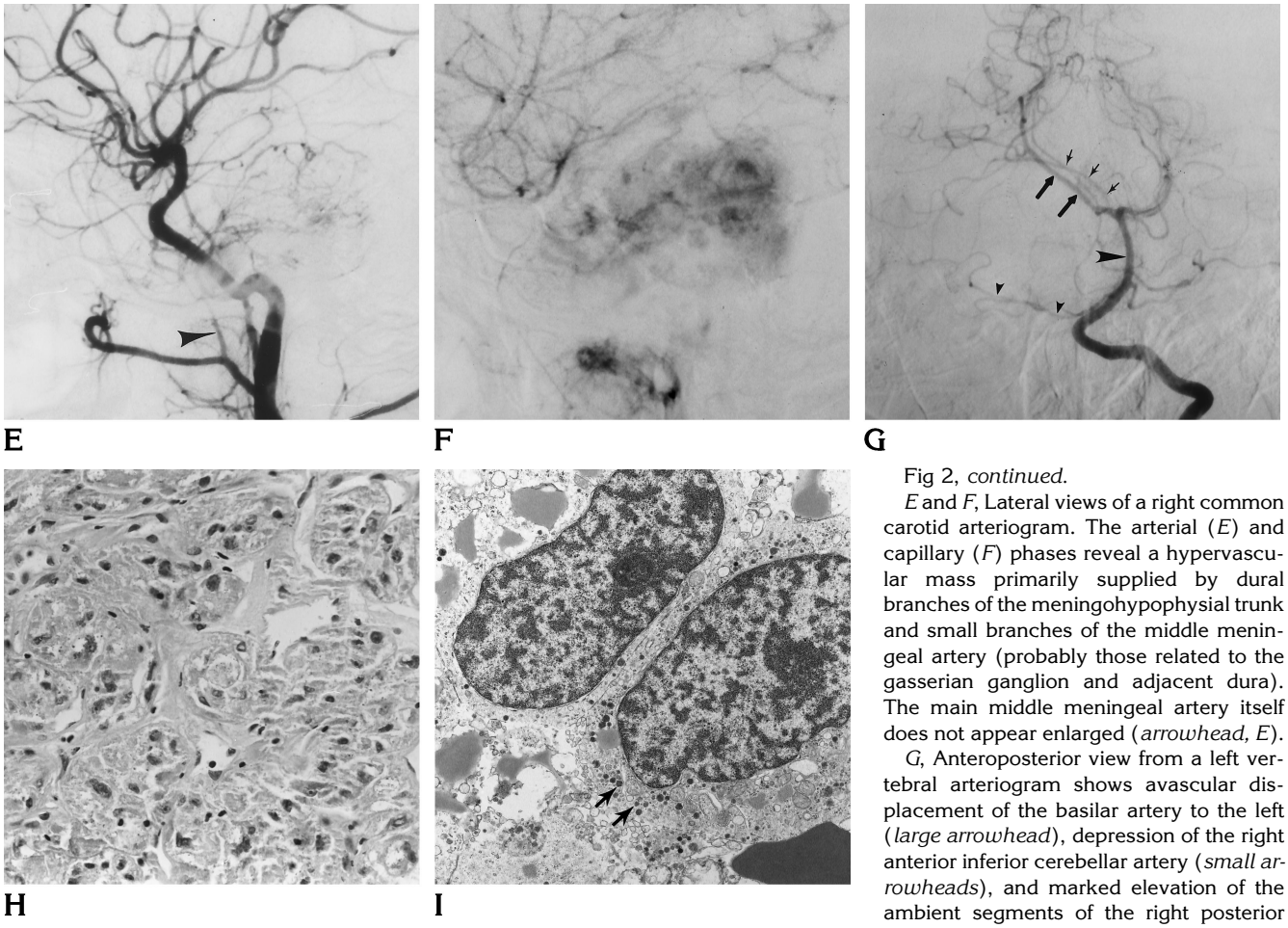

Fig 2, *continued.*

E and *F*, Lateral views of a right common carotid arteriogram. The arterial (*E*) and capillary (*F*) phases reveal a hypervascular mass primarily supplied by dural branches of the meningohypophysial trunk and small branches of the middle meningeal artery (probably those related to the gasserian ganglion and adjacent dura). The main middle meningeal artery itself does not appear enlarged (*arrowhead, E*).

G, Anteroposterior view from a left vertebral arteriogram shows avascular displacement of the basilar artery to the left (*large arrowhead*), depression of the right anterior inferior cerebellar artery (*small arrowheads*), and marked elevation of the ambient segments of the right posterior cerebral (*thick arrows*) and right superior cerebellar arteries (*thin arrows*).

H, Histologic section shows clusters of tumor cells related to vascular spaces (hematoxylin-eosin, original magnification ×240).

I, Electron micrograph shows secretory granules (*arrows*) in tumor cells (×10,500).

cases was based on their histologic appearance, characterized by the arrangement of tumor cells in clusters (zellballen) and their immunoreactivity for chromogranin. Although only a small number of tumor cells showed a positive reaction for chromogranin in case 2, electron microscopy revealed membrane-bound secretory granules characteristically seen in paragangliomas. Because of the parasellar location, we considered the possibility that these tumors might represent aggressive pituitary adenomas, which may sometimes resemble paragangliomas. However, we believe that the tumors in our patients can be distinguished from pituitary adenomas by the total absence of immunoreactivity for major pituitary hormones and, perhaps more important, by the positive staining reaction of the supporting cells for S-100 protein.

These lesions would most certainly be classified as "paragangliomas of uncertain cell origin" (5). Although paraganglionic cells have not been found in the region of the central skull base, Bilbao et al (2) proposed that neural crest tissue may be involved in the development of the pituitary gland and that a nest of paraganglionic tissue may remain in the region of the adenohypophysis. Others have suggested that such tumors may arise from abnormally migrated paraganglionic tissue in the fetus or neonate (6).

References

1. Von Luschka H. Uber de drusenartige natur des sogenanten ganglion intercaroticum. *Arch Anat Physiol* 1862:405
2. Bilbao JM, Horvath E, Kovacs K, Singer W, Hudson AR. Intrasellar paraganglioma associated with hypopituitarism. *Arch Pathol Lab Med* 1978;102:95–98
3. Steel TR, Dailey AT, Born D, Berger MS, Mayberg MR. Paragangliomas of the sellar region: report of two cases. *Neurosurgery* 1993;32:844–847
4. Flint EW, Claassen D, Pang D, Hirsch WL. Intrasellar and suprasellar paraganglioma: CT and MR findings. *AJNR Am J Neuroradiol* 1993;14:1191–1193
5. Russell DS, Rubenstein LJ. *Pathology of Tumors of the Nervous System*. Baltimore, Md: Williams & Wilkins, 1989:692–697
6. Ho KC, Meyer G, Garancis J, Hanna J. Chemodectoma involving the cavernous sinus and semilunar ganglion. *Hum Pathol* 1982; 13:942–943